

# The Overload Behaviour of Reinforced Concrete Flexural Members

Angelo Thurairajah

**Abstract**—Sufficient ultimate deformation is necessary to demonstrate the member ductility, which is dependent on the section and the material ductility. The concrete cracking phase of softening prior to the plastic hinge formation is an essential feature as well. The nature of the overload behaviour is studied using the order of the ultimate deflection. The ultimate deflection is primarily dependent on the slenderness (span to depth ratio), the ductility of the reinforcing steel, the degree of moment redistribution, the type of loading, and the support conditions. The ultimate deflection and the degree of moment redistribution from the analytical study are in good agreement with the experimental results and the moment redistribution provisions of the Australian Standards AS3600 Concrete Structures Code.

**Keywords**—Ductility, softening, ultimate deflection, overload behaviour, moment redistribution.

## NOTATIONS

$a$ & $a_+$	= factors to define concrete crushing (= 1) or steel rupture failure (= 0.75)
$A_s$ & $A_{s+}$	= tension reinforcement at negative & positive moments
$b$ & $d$	= width and effective depth of a section
$f_c'$	= 28th day characteristic strength of concrete
$f_{sy}$	= characteristic yield strength of reinforcement
$f_{su}$	= ultimate rupture strength of reinforcement
$k_1$ & $k_2$	= factors relating to plastic hinge length
$k_3$	= factor relating to plastic hinge rotation capacity
$k_y$ & $k_{y+}$	= neutral axis depth parameters at negative & positive yield moments
$k_u$ & $k_{u+}$	= neutral axis depth parameters at negative & positive ultimate moments
$L$ & $L'$	= span between supports & span excluding plastic hinge zones
$L_s$ & $L_{s+}$	= negative & positive shear spans = $M_u/V_u$ & $M_{u+}/V_{u+}$
$m_u$ & $M_u$	= ultimate negative moment before & after redistribution
$M_{u+}$	= ultimate positive moment after redistribution
$M_y$ & $M_{y+}$	= negative & positive yield moments
$n$ & $n_+$	= negative & positive modular ratios
$p$ & $p_+$	= reinforcement ratios at negative & positive moments
$q$ & $q_+$	= softening indices = inverse of moment-curvature slope change after yield
$r_c$ & $r_p$	= span ratios of contra-flexure from the support & the plastic region at support
$r_y$ & $r_{y+}$	= span ratios of the negative & positive yield moments from the support
$V_u$	= ultimate shear at support
$w_u$	= uniformly distributed load at ultimate limit state
$\alpha_2$	= effective rectangular stress block width coefficient
$\beta$	= degree of moment redistribution

$\gamma$	= effective rectangular stress block depth coefficient
$\Delta_{Re}$	= total empirical midspan deflection capacity
$\Delta_u$	= total analytical midspan deflection at the ultimate limit state
$\Delta_{ui}$	= analytical mid span deflection from the $i^{\text{th}}$ segment at the ultimate limit state
$\epsilon_{cc}$	= concrete crushing strain
$\epsilon_{cu1}$	= concrete strain at the extreme face
$\epsilon_{cu2}$	= concrete strain at $\gamma k_u d$ from the extreme face
$\epsilon_{st}$	= reinforcement rupture strain capacity
$\epsilon_{su}$	= reinforcement strain at the ultimate limit state
$\epsilon_{sy}$	= reinforcement tensile yield strain
$\eta$	= reinforcement over strength ratio = $f_{su}/f_{sy}$
$\phi_{u1}$ & $\phi_{u1+}$	= negative & positive moment curvature at full plasticity
$\phi_{u2}$ & $\phi_{u2+}$	= negative & positive moment curvature at ultimate limit state
$\phi_y$ & $\phi_{y+}$	= negative & positive moment curvature at yield
$\theta_R$ & $\theta_{R+}$	= empirical negative & positive moment plastic rotation capacity
$\theta_{Re}$	= total empirical support rotation capacity
$\theta_u$	= total analytical support rotation at the ultimate limit state
$\theta_{ui}$	= analytical support rotation from the $i^{\text{th}}$ segment at the ultimate limit state

## I. INTRODUCTION

THIS paper follows ‘Ductility and Softening of Reinforced Concrete Flexural Members’ presented at the Concrete 2021 Conference in Australia [1]. The analytical models employed are based on singly reinforced and constant depth internal span (span with fixed ends) concrete flexural member subject to uniform and midspan point loadings with trilinear moment curvature idealization to investigate:

1. The overload behaviour with the ultimate midspan deflection.
2. The moment redistribution provisions of the AS3600 Code.

Concrete is considered a non-ductile material. The higher concrete strength ( $F_c'$ ) and the lack of confinement reduce ductility are illustrated in Fig. 1.

The reinforcement ductility is classified as Class N (Normal) and Class L (Low) in the Australian Standards Concrete Structures Code AS3600 [2]. The ACI318 Code [3] on the other hand does not explicitly account for the material ductility. The ultimate steel rupture strain ( $\epsilon_{st}$ ) and the post-yield over-strength ratio ( $\eta = f_{su}/f_{sy}$ ) influence the reinforcement ductility as illustrated in Fig. 2.

Angelo Thurairajah, Technical Director, is with Webber Design, Australia (e-mail: angthurai@optusnet.com.au).

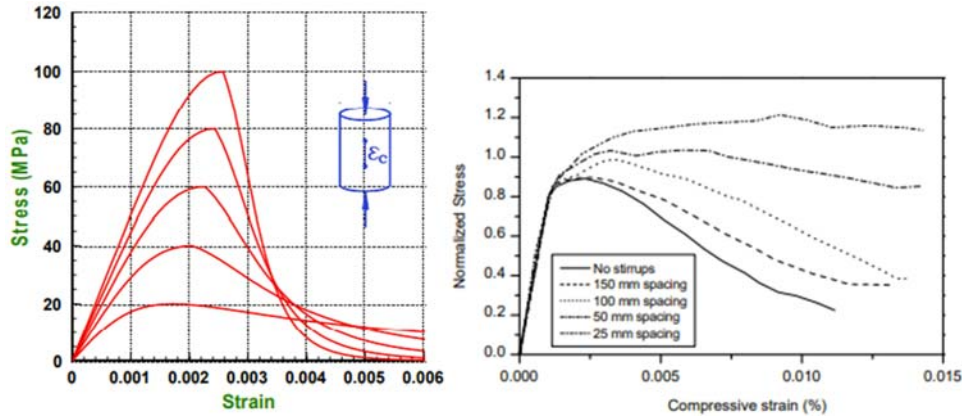


Fig. 1 Material Ductility - Concrete

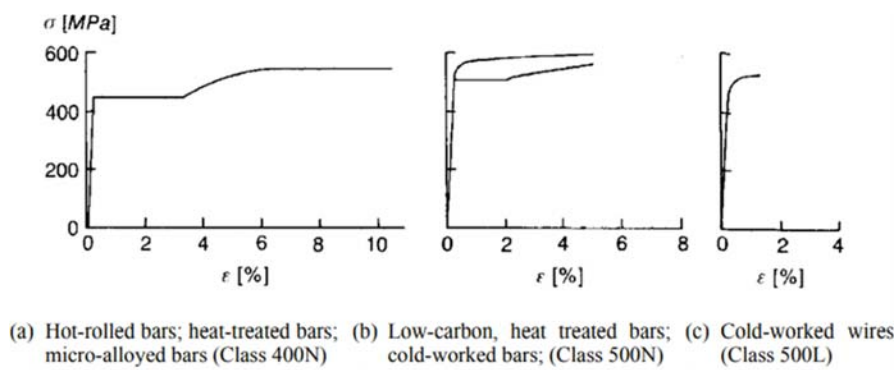


Fig. 2 Material Ductility - Steel

The section ductility is essential for the formation of plastic hinge at a critical section as per [6]. The plastic hinge rotation ductility depends on this, which in turn relies on the material ductility, reinforcement content and the section details. The moment-curvature diagram of Fig. 3 illustrates the ductility of an optimally reinforced section (solid line) and an over-reinforced section (dashed line).

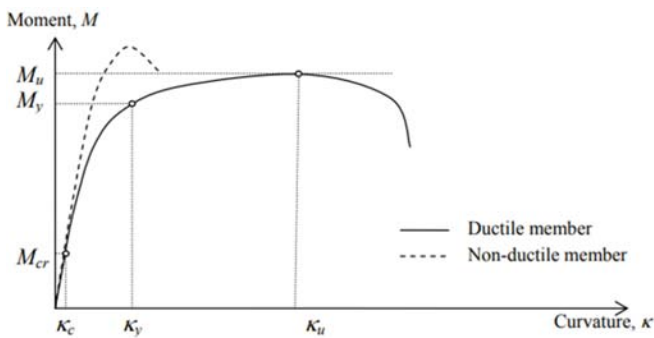


Fig. 3 Section Ductility

The member ductility is essential for the formation of a collapse mechanism with adequate and satisfactory plastic hinges in a redundant flexural member. The member ductility is governed by the section ductility, the span to depth ratio (L/D), the degree of moment redistribution (β), the support conditions and the loading types.

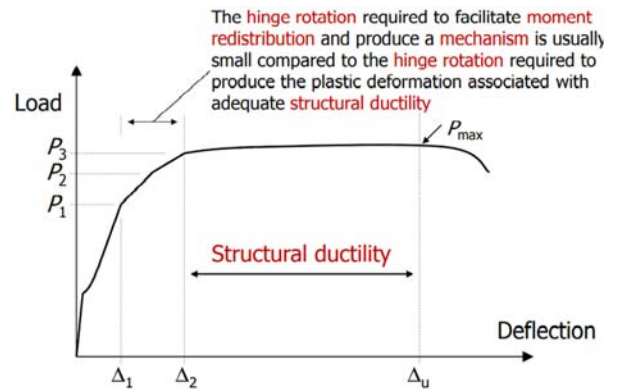


Fig. 4 Member Ductility

The member ductility is illustrated in the load-deflection diagram of Fig. 4.  $\Delta_1$  is the deflection at the first plastic hinge,  $\Delta_2$  is the deflection when the collapse mechanism is formed and  $\Delta_u$  is the ultimate deflection prior to failure.  $\Delta_u/\Delta_2$  defines the structural ductility, and the primary moment redistribution takes place in the region between  $\Delta_1$  and  $\Delta_2$ .

The softening phase with crack formation is another essential characteristic as per [5]. This is represented by line A (less) and line B (more) in the elastic-plastic region 2 in Fig. 5. The softening index (q) is the inverse slope ratios of the yield (region 1) and the softening (region 2).

The ultimate midspan deflection ratio ( $\Delta_u/L$ ) determined analytically is compared with those determined empirically

( $\Delta R_e/L$ ) using the empirical rotation given by [7]. The ultimate midspan deflection ratio ( $\Delta_u/L$ ) against an acceptable limit ( $\Delta R/L$ ) is used as the criteria to determine the nature of the over-load behaviour in this paper.

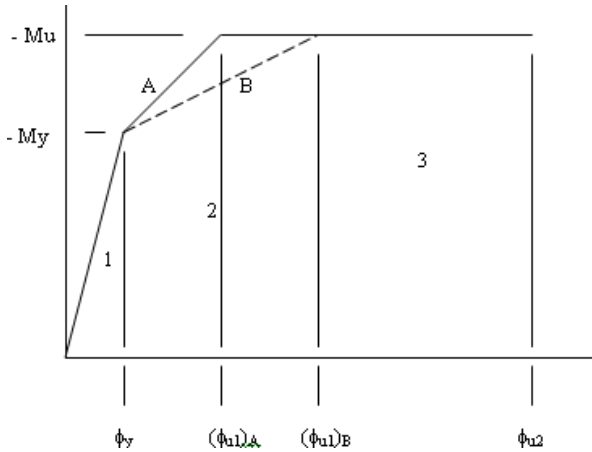


Fig. 5 Softening in Moment-Curvature Diagram

## II. ANALYTICAL MODELS

The analytical models to determine the ultimate midspan deflection ratio ( $\Delta_u/L$ ) of an internal span flexural member with the uniformly distributed load (UDL) and the midspan point load (PL) are summarised in the Appendix.

The internal span requires two negative moment plastic hinges at the supports and a positive moment plastic hinge at midspan to form the collapse mechanism requires the highest deflection demand.

An idealized moment-curvature diagram as illustrated in Fig. 18 in the Appendix includes:

1. Elastic Region: to the yielding of the reinforcement.
2. Softening Region: from yielding of the reinforcement to reaching the ultimate moment.
3. Plastic Region: the constant ultimate moment region where the curvature increases until the concrete spalls or the reinforcement steel is ruptured.

The relationships are established for the plastic, yield & contraflexure span ratios ( $r_p/r_{p+}$ ,  $r_y/r_{y+}$  &  $r_c$ ), the ultimate & yield curvatures ( $\phi_{u1}/\phi_{u2}$ ,  $\phi_{u1+}/\phi_{u2+}$  &  $\phi_y/\phi_{y+}$ ), the ultimate & yield bending moment ratios ( $M_u/M_{u+}$ ,  $M_u/M_y$  &  $M_{u+}/M_{y+}$ ) and the ultimate & yield neutral axis depth parameters ( $k_u/k_{u+}$  &  $k_y/k_{y+}$ ) based on the negative & positive redistributed bending moments and the reinforced concrete engineering principles.

The ultimate deflection ratios ( $\Delta_{ui}/L$ ) for each of the segments described above are obtained from the moment-curvature idealization and summed to obtain the system values ( $\Delta_u/L$ ). The empirical ultimate midspan deflection ratio ( $\Delta R_e/L$ ) is obtained using the empirical rotation estimates of [7].

The service deflection ratio limit in the AS3600 Code is 1/240. Three times of this (1/80) is adopted as the minimum required ultimate deflection. Sakka and Gilbert [4] uses the

ductility factor of 2, which with the over-strength factor of 1.3 gives the ultimate to yield deflection ratio ( $2 \times 1.3 = 2.6$ ) as an acceptable measure.

## III. ANALYTICAL EVALUATIONS

The general observations of the analytical evaluations were described in the paper Ductility and Softening in Reinforced Concrete Flexural Members [1]. Refinements with respect to the failure mode are included in the analytical models.

### A. Rotation

Fig. 6 illustrates an example of the analytical and empirical total ultimate rotations for the whole range of the neutral axis parameter ( $k_u$ ) of an internal span member reinforced with Class N & Class L steel reinforcement subject to UDL loading at moderate degree of moment redistribution ( $\beta = 0.15$ ) and slenderness ( $L/D = 15$ ).

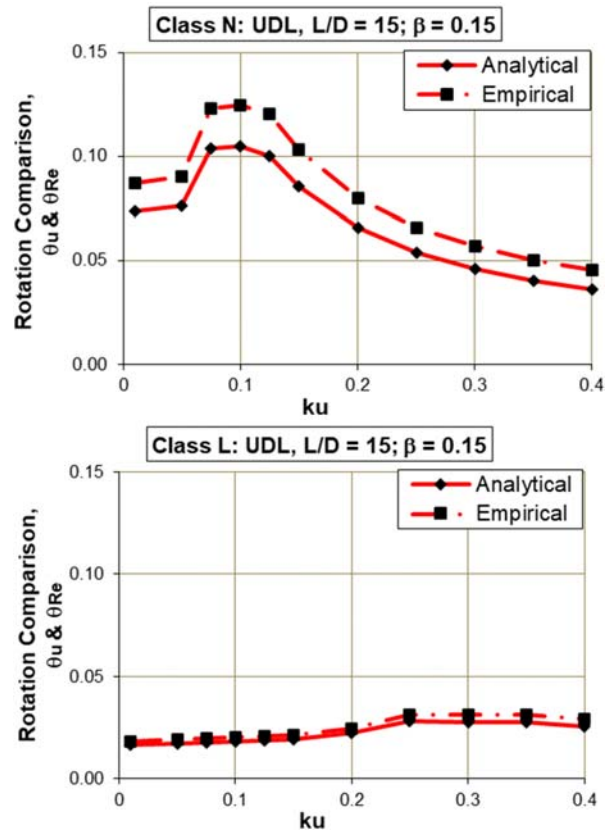


Fig. 6 Typical ultimate rotation comparison - UDL

The estimated rotations are less than those expected from the empirical for the Class N steel but are in close agreement for the Class L steel under both the UDL and PL type of loading.

### B. Ultimate Deflection Ratio

Fig. 7 illustrates that the ultimate analytical deflection ratio ( $\Delta_u/L$ ) increases with the increasing slenderness ( $L/D$ ) for members with both types of reinforcement steel for the UDL load case. The deflection ratio is sufficiently higher than the limit of 1/80 for most of the neutral axis depth parameters ( $k_u$ )

range for the Class N steel. However, the  $\Delta_u/L$  is not sufficient to reach the limit for low the  $L/D$  and  $k_u$  ranges for the Class L steel.

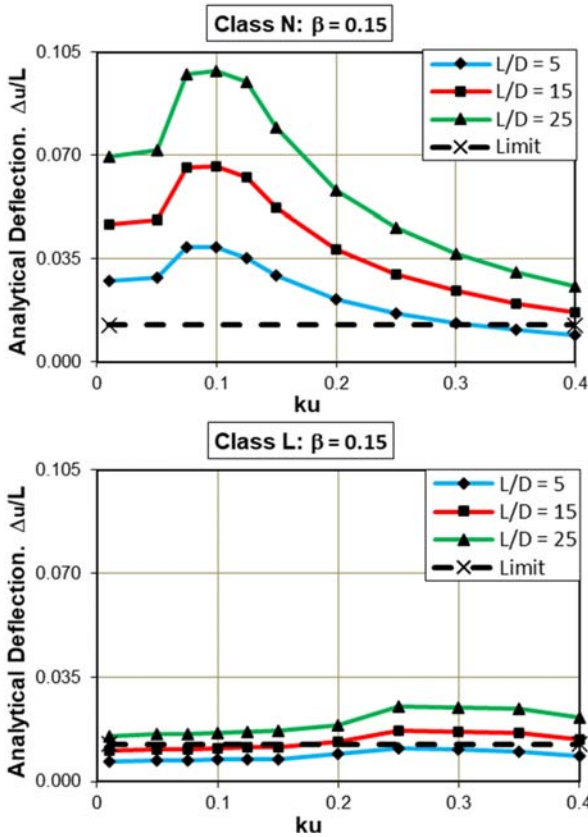


Fig. 7 Ultimate deflection ratio and slenderness - UDL

The ultimate deflection ratio ( $\Delta_u/L$ ) decreases with increasing moment redistribution ( $\beta$ ) for the Class N reinforced member. The variation with respect to the moment redistribution is irregular and not consistent at the set deflection limit for the Class L reinforced member for the UDL load case. The  $\Delta_u/L$  for the PL load case with the Class L steel do not reach the  $L/80$  limit for the full ranges of  $k_u$ ,  $L/D$  and  $\beta$  as in Fig. 8.

Figs. 9 and 10 illustrate examples of the analytical ( $\Delta_u/L$ ) and empirical ( $\Delta_{Re}/L$ ) ultimate deflection ratios for the uniformly distributed (UDL) and the point load (PL) cases. Although of similar trend, the analytical estimation is less for the PL load case. Hence, the midspan point loading case is more critical. Sakka and Gilbert [4] included point loads on two span members and not on the more critical internal span member.

### C. Softening

Fig. 11 illustrates decreasing negative moment softening slope change [ $1/q = (\text{slope } 1 - \text{slope } 2)/(\text{slope } 1)$ ] in Fig. 5 with the increasing neutral axis parameter ( $k_u$ ). It is to be noted that the slope change is greater for the Class L steel than the Class N steel for high  $k_u$  values. The negative moment slope is independent of the moment redistribution ( $\beta$ ), the slenderness ( $L/D$ ) and the type of loading (UDL/PL).

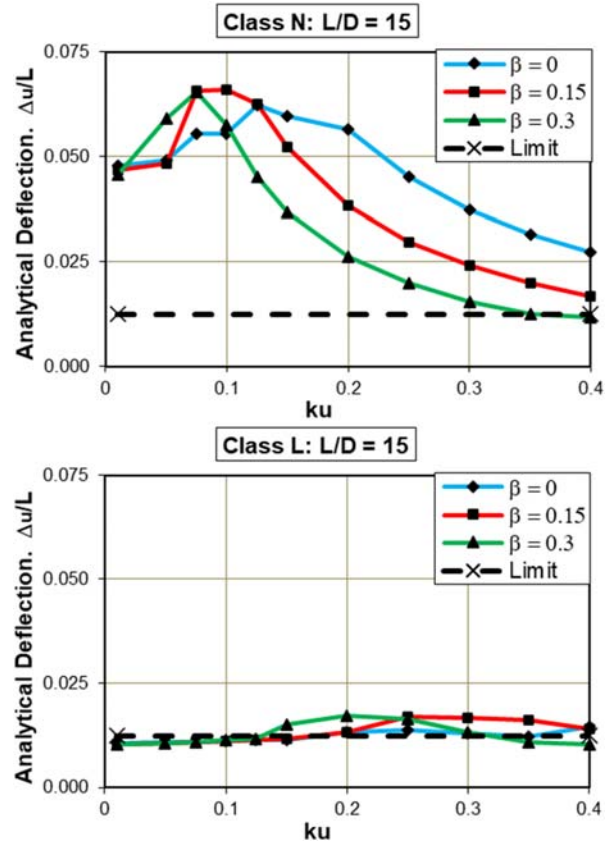


Fig. 8 Ultimate deflection ratio and moment redistribution - internal span - UDL

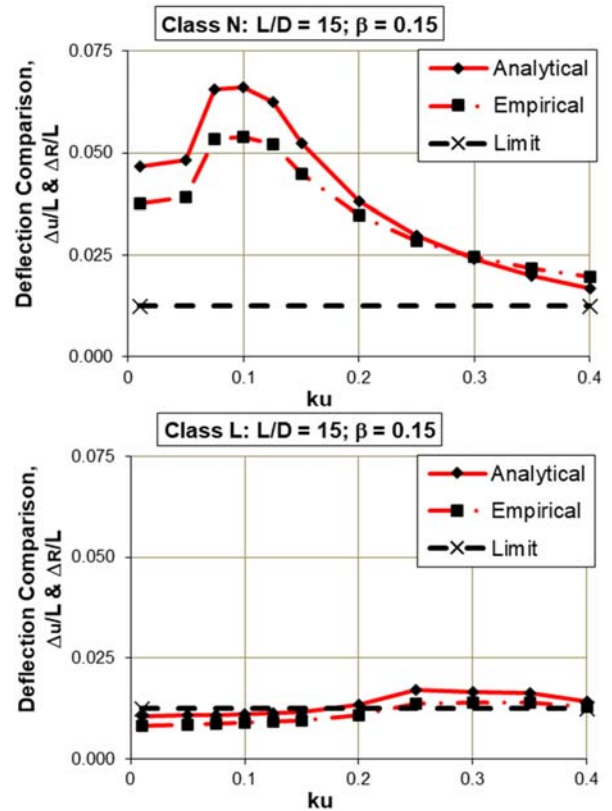


Fig. 9 Typical ultimate deflection ratio comparison - UDL

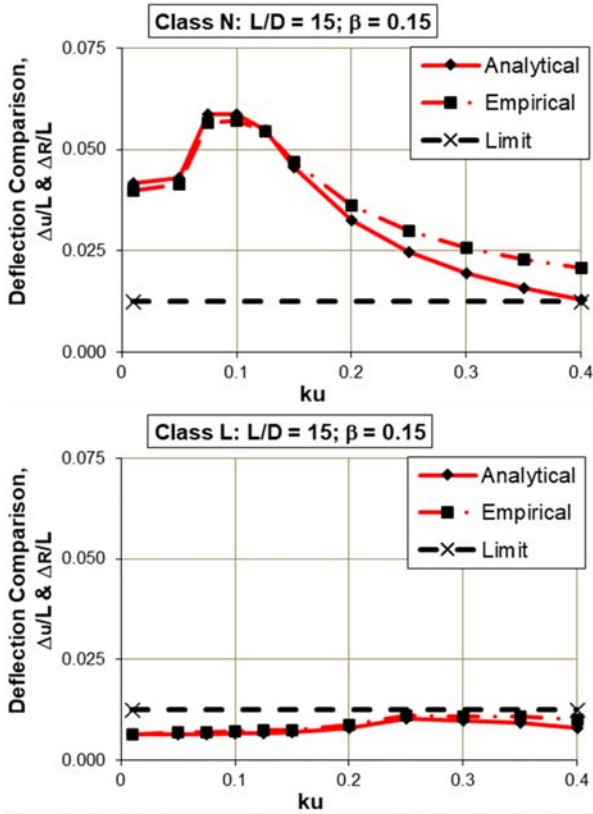


Fig. 10 Typical ultimate deflection ratio comparison - PL

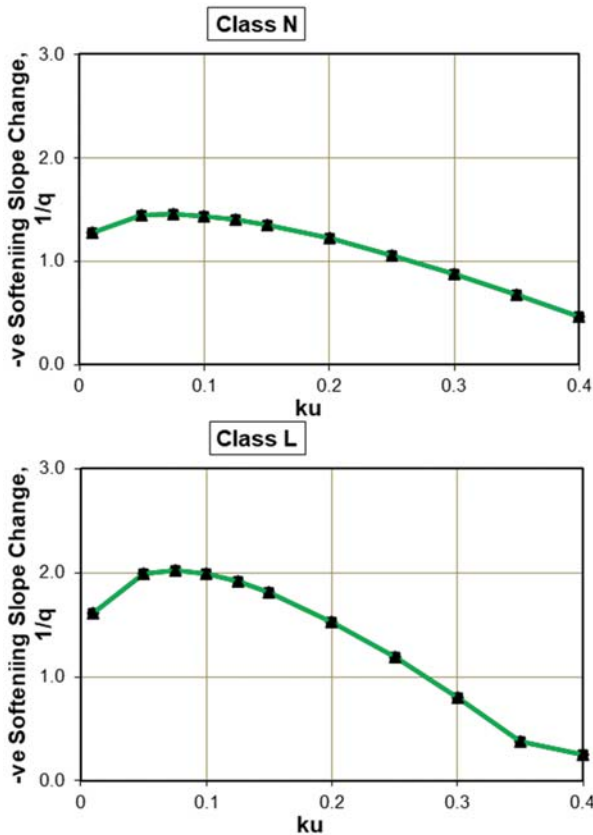


Fig. 11 Negative moment softening slope change

Fig. 12 illustrates decreasing positive moment softening slope change ( $1/q_+$ ) with the increasing neutral axis parameter ( $k_u$ ) for the UDL loading. It is to be noted that the slope change is greater for the Class L steel than the Class N steel for high  $k_u$  values and increases with the  $\beta$ . The positive moment slope is only independent of the slenderness ( $L/D$ ) and the type of loading (UDL/PL).

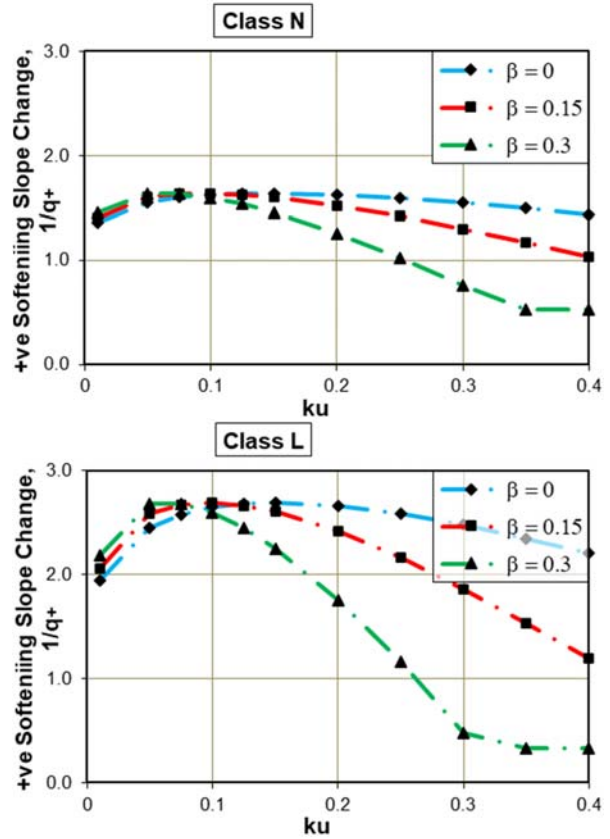


Fig. 12 Positive moment softening slope change

The softening slope changes are indication of crack propagation and plastic hinge formation. Although a good degree of cracked plastic hinge formation is expected in the lower  $k_u$  range, not only the plastic hinges are not likely to display explicit cracking but also are not capable to undergo higher moment redistribution.

#### D. Moment Redistribution

The various degrees of moment redistribution ( $\beta$ ) and the corresponding neutral axis depth parameters ( $k_u$ ) at which the ultimate midspan deflection ratio ( $\Delta_u/L$ ) exceed  $1/80$  with UDL & PL loads at span ratios ( $L/D = 5$  &  $15$ ) of an internal span member in Fig. 13 for the Class N reinforced member. The PL load case is more critical at larger span ratios. AS3600 Code [1] and ACI318 Code [2] provisions are also included for comparison.

The AS3600 Code is too conservative for higher slenderness values. It is appropriate to include this with the following for the Class N steel:

$$k_u = 0 \rightarrow 0.2 \exists \beta = 0.3$$

$$k_u = 0.2 \rightarrow 0.4 \exists \beta = \{0.3 - (k_u - 0.2)[(L/D)/25]\}$$

No feasible  $k_u$  values could be found for any  $\beta$  values for  $L/D = 15$  subject to the PL load case for the Class L reinforced member.

#### IV. EXPERIMENTAL VERIFICATIONS

The published results of [4] are used to verify the parametric study in this paper. 100 mm deep and 1000 mm wide slab strips reinforced with Class N and Class L were used in the experiment as illustrated in Fig. 14.

The material properties of concrete and reinforcement along with the observed ultimate bending moments observed are summarized in Fig. 15.

The degree of moment redistribution ( $\beta$ ) and the ultimate deflection ratio ( $\Delta_u/L$ ) for the four specimens are tabulated against the experimental results in Fig. 16. The formation of the plastic hinges, the mode of failure as to whether concrete spalling or reinforcement rupture and the ultimate deflection ratio are also noted.

#### V. DISCUSSION

##### A. Ductility

The ultimate deflection ratio is found to depend on the degree of moment redistribution, the slenderness, the neutral axis depth parameter, the ductility of reinforcing steel, the support rotation fixity (pinned/ fixed) and the type of loading (UDL/PL). The ultimate analytical deflection ratio agrees with the empirical estimate based on [7] at high neutral axis parameter for the UDL

loading and at low neutral axis parameter for the PL loading.

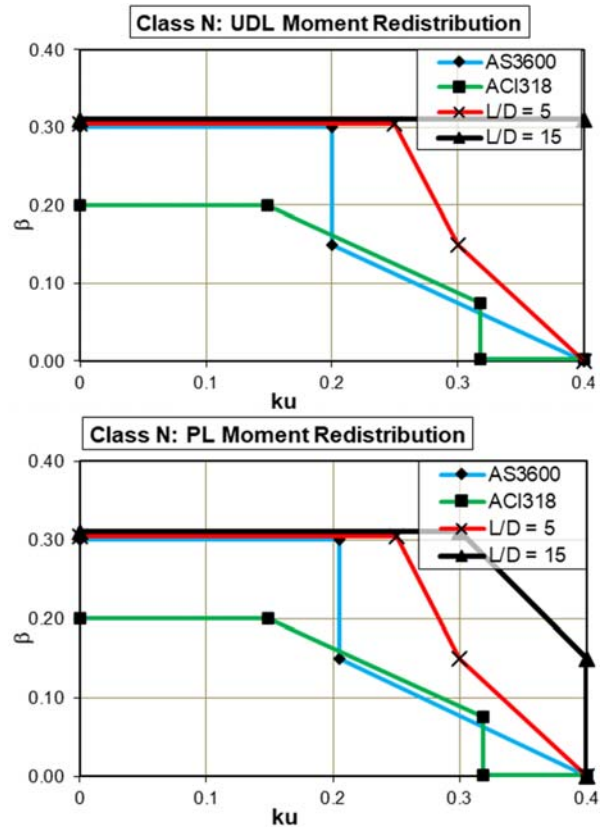


Fig. 13 Moment redistribution - Class N

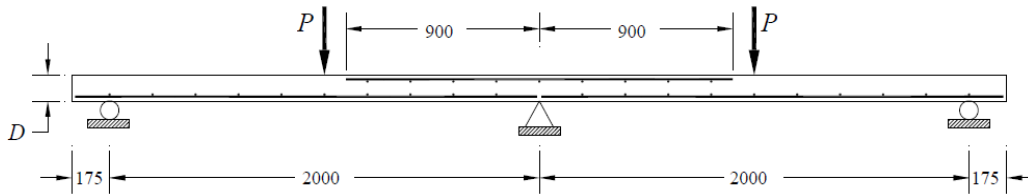


Fig. 14 Geometry and Loading Configuration of the Experiments

Specimen No	L/D	As	As+	fc	Fsy/ Fsy+	$\eta/\eta+$	$\epsilon_{cu}$	$\epsilon_{su}/\epsilon_{su+}$	Mu	Mu+
		mm <sup>2</sup>	mm <sup>2</sup>	MPa	MPa				kNm	kNm
CS3	20	227	227	37.8	581/581	11.10/1.10	0.0030	0.024/0.024	-11.0	11.0
CS4	20	354	227	37.8	578/615	1.08/1.07	0.0030	0.033/0.019	-14.0	11.0
CS5	20	339	339	37.8	591/591	1.15/1.15	0.0030	0.098/0.098	-15.5	15.5
CS11N	20	141	227	47.5	586/597	1.07/1.04	0.0030	0.036/0.030	-9.5	12.0

Fig. 15 Experimental data and results

Specimen No	AS3600 Class	Experiment		Analytical		Hinges Formed	Mode of Failure	Ultimate Deflection
		$\Delta$	$\beta$	$\Delta$	$\beta$			
		mm	%	mm	%			
CS3	L	24.2	10	25.0	7	Both	Bottom steel rupture	= L/80
CS4	L	24.9	5	25.0	5	Nearly both	Bottom steel rupture	= L/80
CS5	N	95.1	12	105.0	15	Both	Concrete spalling	= L/20
CS11N	L	26.0	20	30.0	12	Both	Top steel rupture	= L/67

Fig. 16 Comparison of Results

Adequate member ductility is achieved when the ultimate deflection ratio exceeds 1/80. Elements with lower neutral axis depth parameter indicate higher ductility but those under-reinforced ended with premature steel rupture and those over-reinforced failed without adequate steel deformation. The Class N reinforcement renders sufficient ductility at most cases while the Class L reinforced member was brittle. There is lack of redundancy with limited displacement capacity of the Class L reinforcement.

### B. Softening

The cracking process during softening acts as a warning indicator prior as the critical section reaches the ultimate moment prior to the formation of the plastic hinge. However, extensive softening reduces the available ductility of a section as illustrated in Fig. 5.

The section with higher neutral axis depth parameter demonstrates lower softening at increased degree of moment redistribution for the Class N reinforced member. This effect is more profound on the Class L reinforced member as seen in the experimental observation by not developing extensive cracking as a warning sign during the overload regime.

### C. Moment redistribution

The allowable degree of moment redistribution is determined in this paper when the ultimate midspan deflection is sufficient for a ductile behaviour. The estimations from the analytical procedure are in reasonable agreement with the experiment of [4].

The parametric studies and the experimental results presented demonstrate that the AS3600 Code [1] deemed-to-comply moment redistribution for Class N reinforced member is agreeable at low slenderness but is conservative at high slenderness. Hence the findings here align with the AS Code deemed to comply section in restricting the use of Class L steel.

### D. Research Significance

The ultimate deflection describes the overload behaviour of reinforced concrete flexural member well. This method is useful to investigate the overload behaviour of different characteristics of reinforcement, slenderness ratios etc.

An extension of this study should benefit the lateral structure design with Performance Based Design (PBD) techniques which impose greater emphasis on the overload behaviour.

## VI. CONCLUSION

Based on the results of the parametric studies, the experiment and the discussion above:

1. *Ductility* is measured by the ultimate mid span deflection and is dependent on the degree of moment redistribution, the slenderness ratio, the neutral axis depth parameter, the ductility of reinforcement, the support types and the type of loading. The Class N reinforced member is ductile while the Class L reinforced is brittle without redundancy.
2. *Softening* is the cracking process prior to the plastic hinge formation. The Class N reinforcement renders sufficient softening characteristics at low neutral axis depths.

3. *Moment redistribution* related clauses of the AS3600 Code [1] is generally in agreement for the Class N reinforcement for short slenderness but appear to be conservative for long slenderness. The exclusion of Class L reinforcement in the deemed to comply provision of the Code is justified.

## APPENDIX

Fig. 17 illustrates the loading and the bending moment diagrams with the negative moments before & after redistribution  $-m_u$  &  $-M_u$  and midspan positive moment  $M_+$  after redistribution for an internal span member with uniformly distributed load  $w_u$ .

$$m_u = w_u L^2 / 12 \xrightarrow{\text{results}} M_u = (1 - \beta)m_u \text{ and } M_{u+} = \left(\frac{1}{2} + \beta\right)m_u \quad (1)$$

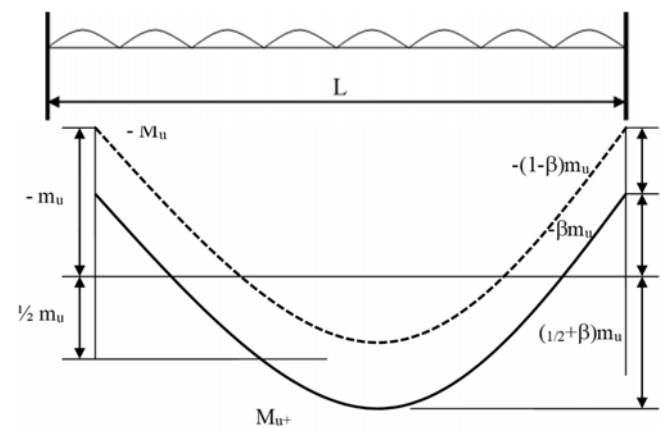


Fig. 17 Bending moment diagram of an internal span

Equation (1) reduces to:

$$M_{u+} / M_u = \left[ \left( \frac{1}{2} + \beta \right) / (1 - \beta) \right] \quad (2)$$

Idealized moment-curvature and detailed bending moment diagrams are illustrated in Fig. 18 along a half span.  $M_x$  is the bending moment at a distance 'x' from the centre of the span.

Bending moment in between the negative and positive plastic hinges:

$$M_x = M_{u+} - w_u x^2 / 2 \xrightarrow{\text{results}} M_x = \left\{ \left[ \left( \frac{1}{2} + \beta \right) - 6 \left( \frac{x}{L} \right)^2 \right] / (1 - \beta) \right\} M_u \quad (3)$$

Shear at the end span  $V_u = w_u L / 2$ , and the negative moment shear-span:

$$L_s / L = M_u / V_u = (1 - \beta) / 6$$

Shear at the mid span  $V_+ \rightarrow 0$ , with  $L_{s+} < 0.5L$  and the positive moment shear-span:

$$L_{s+} / L = M_{u+} / V_{u+} \rightarrow 0.5 \quad (4)$$

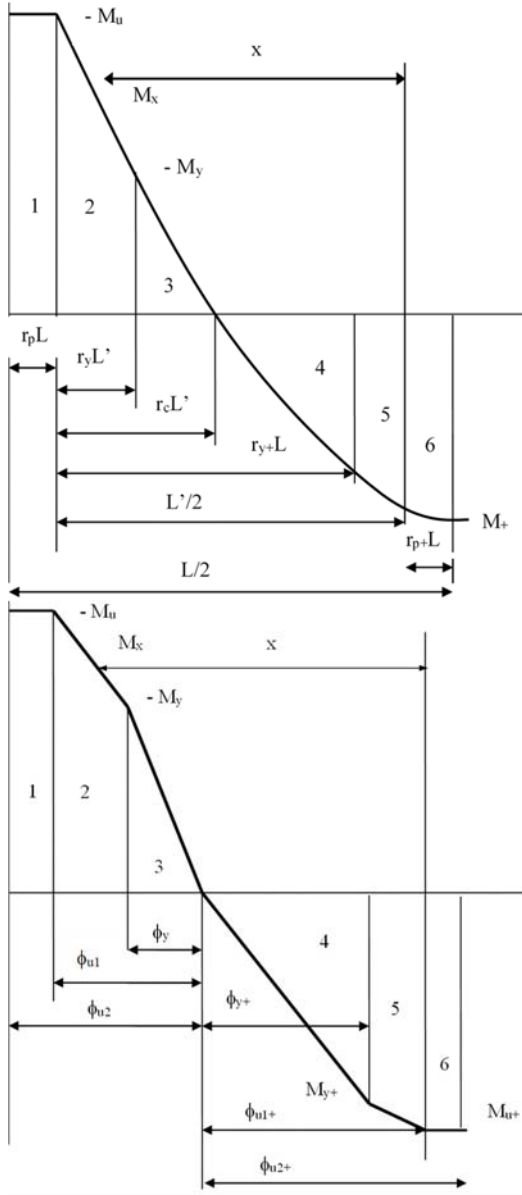


Fig. 18 Detailed bending moment diagram and idealized moment curvature diagram

The negative moment plastic, yield & contra-flexure span ratios  $r_p$ ,  $r_y$ ,  $r_c$  and the positive moment yield ratio  $r_{y+}$  are summarized by (5)-(8).

From [7],  $k_1 = 0.15$  &  $0.1$  and  $k_2 = 0.18$  &  $0.15$  for Class N and Class L reinforcement respectively:

$$r_p = \text{Maximum}[(d/L + k_1 r_c)/2; k_2 L_s] \quad (r_{p+} \text{ is similar}) \quad (5)$$

$$x = (\frac{1}{2} - r_y)L' \rightarrow M_x = -M_y \rightarrow r_y = \langle \frac{1}{2} - \sqrt{\{[(\frac{1}{2} + \beta) + (1 - \beta)(M_y/M_u)]/6\}} \quad (6)$$

$$x = (\frac{1}{2} - r_c)L' \rightarrow M_x = 0 \rightarrow r_y = \langle \frac{1}{2} - \{[(\frac{1}{2} + \beta)]^{1/2}/6\} \quad (7)$$

$$x = (\frac{1}{2} - r_{y+})L' \rightarrow M_x = M_{y+} \rightarrow$$

$$r_{y+} = \langle \frac{1}{2} - \{[(\frac{1}{2} + \beta)(1 - M_{y+}/M_u)]^{1/2}/6\} \quad (8)$$

With  $L' = (1 - 2r_p - 2r_{p+})L$ ;

The negative moment ultimate rotation in segment 1 of Fig. 19 due to the plastic rotation from curvature ( $\phi_{u1}$  to  $\phi_{u2}$ ):

$$\theta_{u1} = [(\phi_{u2} - \phi_{u1})r_p/(1 - 2r_p - 2r_{p+})]L'$$

The peak deflection due to the plastic rotation:

$$\Delta_{u1}/L' = \theta_{u1}(1 - r_p - r_{p+})L/2 \rightarrow \Delta_{u1} = [(\phi_{u2} - \phi_{u1})r_p(1 - r_p - r_{p+})/(1 - 2r_p - 2r_{p+})^2]L'/2 \quad (9)$$

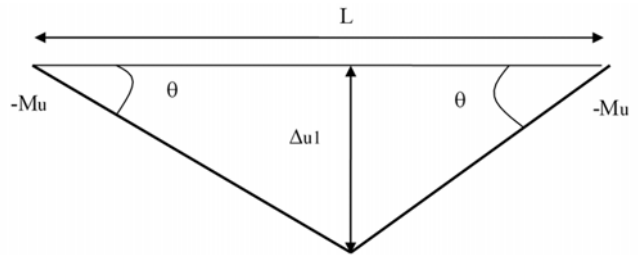


Fig. 19 Plastic rotation of an internal span

M- $\phi$  slopes in segments 2 to 5 of Fig. 18:

$$\begin{aligned} (\text{Slope})_2 &= (M_x + M_y)/(\phi_x - \phi_y) \ni \phi_x = \phi_u \rightarrow M_x = -M_u \\ (\text{Slope})_3 &= (M_x)/(\phi_x) \ni \phi_x = \phi_y \rightarrow M_x = -M_y \\ (\text{Slope})_4 &= (M_x)/(\phi_x) \ni \phi_x = \phi_{y+} \rightarrow M_x = -M_{y+} \\ (\text{Slope})_5 &= (M_x - M_{y+})/(\phi_x - \phi_{y+}) \ni \phi_x = \phi_{u+} \rightarrow M_x = M_{u+} \\ q &= (\phi_{u1}/\phi_y - 1)/(M_u/M_y - 1) \ \& \ q_+ = (\phi_{u1+}/\phi_{y+} - 1)/(M_{u+}/M_{y+} - 1) \quad (10) \end{aligned}$$

Support rotation and maximum in span deflection due to segment 'i' are:

$$\theta_{ui} = \int (\phi_x) \partial x \ \& \ \Delta_{ui} = \int (\phi_x) \partial x \partial x \ni i = 2 \rightarrow 5$$

M- $\phi$  slope in segment 2 with:

$$\begin{aligned} x &\in [(\frac{1}{2} - r_y)L' \rightarrow \frac{1}{2}L'] \\ \phi_x &= \{(1 - q) - [q/(1 - \beta)]\}[(\frac{1}{2} + \beta) - 6(x/L')^2](M_u/M_y)\phi_y \\ \theta_{u2} &= \{(1 - q) + [q/(1 - \beta)]\}[(1 - \beta) - r_y(3 - 2r_y)](M_u/M_y)\phi_y L' \\ \Delta_{u2}/L' &= \{(1 - q) - [q/(1 - \beta)]\}[(\beta) + r_y(1 - r_y)](M_u/M_y)r_y(1 - r_y)\phi_y L'/2 \quad (11) \end{aligned}$$

M- $\phi$  slope in segment 3 with:

$$\begin{aligned} x &\in [(\frac{1}{2} - r_c)L' \rightarrow (\frac{1}{2} - r_y)L'] \\ \phi_x &= -\{[(\frac{1}{2} + \beta) - 6(x/L')^2]/(1 - \beta)\}(M_u/M_y)\phi_y \\ \theta_{u3} &= \{[(1 - \beta) - r_y(3 - 2r_y) - r_c(3 - 2r_c) + 2r_y r_c]/(1 - \beta)\}(M_u/M_y)(r_c - r_y)\phi_y L' \\ \Delta_{u3}/L' &= -\{[\beta + r_y(1 - r_y) + r_c(1 - r_c)]/(1 - \beta)\}(M_u/M_y)(r_c - r_y)(1 - r_c - r_y)\phi_y L'/2 \quad (12) \end{aligned}$$

M-φ slope in segment 4 with:

$$\begin{aligned} x &\in \left[\left(\frac{1}{2} - r_{y+}\right)L' \rightarrow \left(\frac{1}{2} - r_c\right)L'\right] \\ \varphi_x &= -\left\{\left[\left(\frac{1}{2} + \beta\right) - 6(x/L')^2\right]/\left(\frac{1}{2} + \beta\right)\right\}(M_{u+}/M_{y+})\varphi_{y+} \\ \theta_{u4} &= \left\{\left[-(1 - \beta) + r_c(3 - 2r_c) + r_{y+}(3 - 2r_{y+}) + 2r_cr_{y+}\right]/\left(\frac{1}{2} + \beta\right)\right\}(M_{u+}/M_{y+})(r_{y+} - r_c)\varphi_{y+}L' \\ \Delta_{u4}/L' &= -\left\{\left[\beta + r_c(1 - r_c) + r_{y+}(1 - r_{y+})\right]/\left(\frac{1}{2} + \beta\right)\right\}\left(\frac{M_{u+}}{M_{y+}}\right)(r_{y+} - r_c)(1 - r_c - r_{y+})\varphi_{y+}L'/2 \quad (13) \end{aligned}$$

M-φ slope in segment 5 with:

$$\begin{aligned} x &\in \left[0 \rightarrow \left(\frac{1}{2} - r_{y+}\right)L'\right] \\ \varphi_x &= \left\{(1 - q_+) + \left[q_+/\left(\frac{1}{2} + \beta\right)\right]\left[\left(\frac{1}{2} + \beta\right) - 6(x/L')^2\right]\right\}(M_{u+}/M_{y+})\varphi_{y+} \\ \theta_{u5} &= \left\{(1 - q_+) + \left[q_+/\left(\frac{1}{2} + \beta\right)\right]\left[\left(\frac{1}{2} + \beta\right) - 2\left(\frac{1}{2} - r_{y+}\right)^2\right]\right\}(M_{u+}/M_{y+})\left(\frac{1}{2} - r_{y+}\right)\varphi_{y+}L' \\ \Delta_{u5}/L' &= \left\{(1 - q_+) + \left[q_+/\left(\frac{1}{2} + \beta\right)\right]\left[\left(\frac{1}{2} + \beta\right) - \left(\frac{1}{2} - r_{y+}\right)^2\right]\right\}(M_{u+}/M_{y+})\left(\frac{1}{2} - r_{y+}\right)^2L'/2 \quad (14) \end{aligned}$$

The positive moment ultimate rotation in segment 6 from curvature ( $\varphi_{u1+}$  to  $\varphi_{u2+}$ ):

$$\begin{aligned} \theta_{u6} &= [(\varphi_{u2} - \varphi_{u1})r_{p+}/(1 - 2r_p - 2r_{p+})]L' \\ \Delta_{u6}/L' &= [(\varphi_{u2+} - \varphi_{u1+})r_{p+}(1 - r_p - r_{p+})/(1 - 2r_p - 2r_{p+})^2]L'/2 \quad (15) \end{aligned}$$

The analytical total ultimate support rotation and midspan deflection are the sums of segments 1 to 6 from (9)-(15) with (24) for  $a$  and  $a_+$ ;

$$\theta_u = \sum(a/a_+)\theta_{ui} \quad \& \quad \Delta_u = \sum(a/a_+)\Delta_{ui}; \quad i = 1 \rightarrow 6 \quad (16)$$

Equations (17)-(20) relate  $k_u$  to  $k$  &  $k_{u+}$  and  $M_u/M_y$  to  $M_{u+}/M_{y+}$ .

Negative and positive moment region reinforcement ratios:

$$p = [(\alpha_2 f_c')/(\eta f_{sy})]k_u \quad \& \quad p_+ = [(\alpha_2 f_c')/(\eta f_{sy})]k_{u+} \quad (17)$$

Negative and positive moment region yield neutral axis parameters are:

$$k_y = [(np)^2 + (2np)]^{1/2} - (np) \quad \& \quad k_{y+} = [(np_+)^2 + (2np_+)]^{1/2} - (np_+) \quad (18)$$

Ultimate and yield moment capacities at the support (and similar at mid-span);

$$\begin{aligned} M_u &= pb\eta f_{sy} d^2 (1 - \gamma k_u/2) \quad \& \quad M_y = pb f_{sy} d^2 (1 - k_y/3) \\ M_u/M_y &= \eta(1 - \gamma k_u/2)/(1 - k_y/3) \quad \& \quad M_{u+}/M_{y+} = \eta(1 - \gamma k_{u+}/2)/(1 - k_{y+}/3) \quad (19) \end{aligned}$$

The ultimate positive to negative moment ratios:

$$M_{u+}/M_u = (k_{u+}/k_u)(1 - \gamma k_{u+}/2)/(1 - \gamma k_u/2) \rightarrow$$

$$k_{u+} = \left\{1 - [2\gamma k_u(1 - \gamma k_u/2)(\frac{1}{2} + \beta)/(1 - \beta)]^{1/2}\right\}/\gamma \quad (20)$$

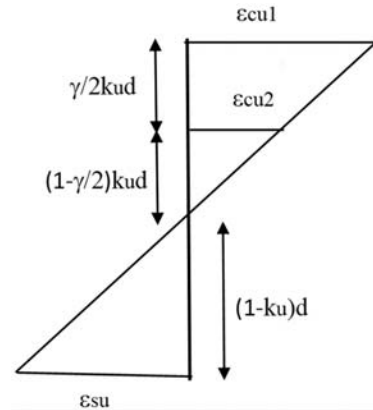


Fig. 20 Strain diagram

The concrete ultimate crushing strain  $\epsilon_{cu1}$ , the ultimate concrete spalling strain  $\epsilon_{cu2}$  and the ultimate steel strain  $\epsilon_{su}$  are summarized with their respective depths in Fig. 20.

The negative and positive yield curvatures:

$$\varphi_y = \epsilon_{sy}/[(1 - k_y)]d \quad \& \quad \varphi_{y+} = \epsilon_{sy+}/[(1 - k_{y+})]d \quad (21)$$

The negative and positive moment curvatures at the onset of plasticity with concrete crushing:

$$\begin{aligned} \varphi_{u1} &= \text{Min}\{\epsilon_{cu1}/(k_u d), \quad \eta \epsilon_{sy} [(1 - k_y)]d\} \quad \& \\ \varphi_{u1+} &= \text{Min}\{\epsilon_{cu1}/(k_{u+} d), \quad \eta \epsilon_{sy+}/[(1 - k_{y+})]d\} \quad (22) \end{aligned}$$

The negative and positive moment curvatures at the ultimate limit state with reinforcement rupture or concrete spalling with concrete crushing occurring at the mid-depth of the rectangular concrete stress block of  $(1 - \gamma/2)k_u d$ :

$$\begin{aligned} \varphi_{u2} &= \text{Min}\{\epsilon_{su}/[(1 - k_u)], \quad \epsilon_{cu2}/[(1 - \gamma/2)k_u d]\} \quad \& \\ \varphi_{u2+} &= \text{Min}\{\epsilon_{su+}/[(1 - k_{u+})], \quad \epsilon_{cu2}/[(1 - \gamma/2)k_{u+} d]\} \quad (23) \end{aligned}$$

The empirical support rotation capacity available given by [7]:

$$\begin{aligned} \theta_R &= a[(\varphi_{u2} - \varphi_{u1})r_p L + k_3] \\ \theta_R &= a\{(\varphi_{u2} - \varphi_{u1})r_p L [1 - 0.5r_p(L/L_s)] + \varphi_{u1}L_s/3\} \quad (24) \end{aligned}$$

$k_3 = 0.005$  and  $0.0025$  for Class N and Class L reinforcement respectively. Similar for  $\theta_{R+}$ .

$a$  &  $a_+$  are defined as 1 for the rupture of the reinforcement at the negative and positive moment regions to occur after the onset of concrete crushing:

$$\begin{aligned} \epsilon_{cu1} &= \epsilon_{cc} \quad \text{when} \quad \epsilon_{su} \leq \epsilon_{st} \rightarrow a = 1 \quad \& \quad a \\ &= 0.75 \quad \text{otherwise} \\ \epsilon_{cu1+} &= \epsilon_{cc} \quad \text{when} \quad \epsilon_{su+} \leq \epsilon_{st} \rightarrow a_+ = 1 \quad \& \quad a_+ \\ &= 0.75 \quad \text{otherwise} \quad (25) \end{aligned}$$

where,  $\epsilon_{cc} = 0.003$  in AS3600.

$a$  and  $a_+$  are 1 for ductile 0.75 for brittle conditions. The proportion of the brittle (Class L) to ductile (Class N) capacity reduction factors in the AS Code [1] is  $0.65/0.85 = 0.75$ .

The total empirical support rotation and deflection  $\theta_R$  and  $\Delta_R$  with the reduction factor  $c_r$  applied to the deflection capacity:

$$\theta_{Re} = c_r(a\theta_R + a_+\theta_{R+}) \text{ and } \Delta_{Re}/L = \theta_{Re}(1 - r_p - r_{p+})/2 \quad (26)$$

Equation (26) is the equivalents of the analytical rotation and deflection from (16).

The degree of moment redistribution ( $\beta$ ) in cl.6.2.7.2 of AS3600 [1] is summarized as:

$$\begin{aligned} \text{Class N: } k_u \leq 0.2 \rightarrow \beta = 0.3, 0.2 < k_u < 0.4 \rightarrow \beta \\ = 0.75(0.4 - k_u) \text{ \& } k_u = 0.4 \rightarrow \beta = 0 \\ \text{Class L: } \beta = 0 \end{aligned} \quad (27)$$

The moment redistribution in cl.8.4 of ACI 318 [2] is summarized as:

$$\varepsilon_{su} < 0.0075 \rightarrow \beta = 0 \text{ and } \beta = \text{Maximum}(10\varepsilon_{su}, 0.02) \quad (28)$$

#### REFERENCES

- [1] Thurairajah A, 2021, Ductility and Softening of Reinforced Concrete Flexural Members, Concrete 2021 Digital Conference, Concrete Institute of Australia.
- [2] AS3600-2018, Concrete Structures Code, Standards Association of Australia.
- [3] ACI 318 - 2014, Concrete Structures Code & Commentary, American Concrete Institute.
- [4] Sakka Z & Gilbert R, 2009, Impact of Steel Ductility on the Structural Behaviour and Strength of RC Slabs, PhD Thesis, UNSW, Sydney, Australia.
- [5] Warner R, 2004, Overload Behaviour of Concrete Structures: Design Considerations, Australian Journal of Structural Engineering, V.5, No.2.
- [6] Gravina R & Warner R, 2003, Evaluation of the AS3600 Design Clauses for Moment Redistribution and Ductility Levels, Australian Journal of Structural Engineering, V.5, No.1.
- [7] Telemachos B, Panagiotakos T and Fardis M, 2001, Deformations of Reinforced Concrete Members at Yielding and Ultimate, ACI Structural Journal, V.98, No.13.